

Electrochemistry

DOI: 10.1002/ange.200602891

**Redox Targeting of Insulating Electrode Materials: A New Approach to High-Energy-Density Batteries\*\***

*Qing Wang, Shaik M. Zakeeruddin, Deyu Wang, Ivan Exnar, and Michael Grätzel\**

Electrochemical devices are currently under intense investigation for sustainable and environmentally benign electric-energy production and storage. The surge of portable

[\*] Dr. Q. Wang,<sup>[†]</sup> Dr. S. M. Zakeeruddin, Dr. D. Wang, Prof. M. Grätzel  
Laboratoire de photonique et interfaces  
Ecole Polytechnique Fédérale de Lausanne  
1015 Lausanne (Switzerland)  
Fax: (+41) 216-936-100  
E-mail: michael.gratzel@epfl.ch  
Homepage: <http://isic2.epfl.ch/page58671.html>  
Dr. I. Exnar  
HPL SA  
1015 Lausanne (Switzerland)

[†] Current address:  
National Renewable Energy Laboratory (USA)

[\*\*] We acknowledge financial support of this work by a CTI project (contract No. 7136.3 EPRP-IW). We thank Dr. H. Li at the Institute of Physics, Chinese Academy of Sciences, for the kind help of making the carbon-free LiFePO<sub>4</sub> sample.



Supporting information for this article is available on the WWW under <http://www.angewandte.org> or from the author.

consumer electronics has galvanized research on portable high-capacity power sources. Improvement of the energy density in electrochemical power sources ranging from conventional lead–acid batteries through to Ni–Cd, Ni–MH, and the state-of-the-art lithium-ion batteries has been a key issue for the past several decades.<sup>[1,2]</sup> The electroactive materials must be electrochemically addressable for their capacity to be explored fully. However, owing to a lack of electronic conductivity of the electrode material, a large amount of conducting additive, such as carbon black, has to be incorporated into the electrode sheet to form a continuous conducting network for electron percolation.<sup>[3,4]</sup> Consequently, the energy density of the battery is greatly decreased by the presence of a large volume of inactive conducting agent.

Molecular wiring of poorly conducting battery materials promises to reduce the need for carbon addition.<sup>[5]</sup> In this case, the charges are transported from the current collector through a molecular layer adsorbed at the surface of the lithium-intercalating particles. As the molecular relay is chosen such that its Nernst potential matches the Fermi level of the substrate, interfacial charge transfer coupled to lithium release or insertion takes place, thus resulting in charging or discharging of the electrode material. Although intriguing, molecular wiring can have stability problems because of the possibility of desorption of the redox mediator from the insertion material during the charge and discharge cycle. Furthermore, the current output is limited by the rate of cross-surface charge percolation and interfacial charge transfer.

Herein we introduce redox targeting by freely diffusing relay molecules to address insulating or poorly conducting lithium-insertion materials. To our knowledge this approach has not been described previously. Figure 1 illustrates the

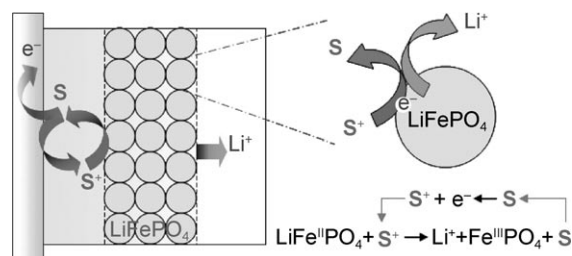
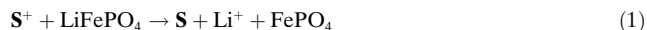


**Figure 1.** The principle of redox targeting of an insulating electrode material such as LiFePO<sub>4</sub> by a freely diffusing molecular shuttle **S**.

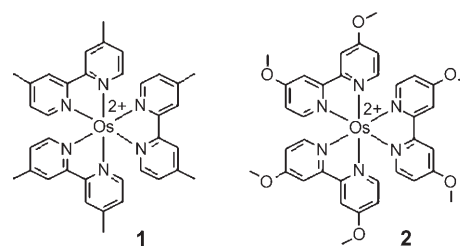
principle of the method by using as an example LiFePO<sub>4</sub>, a large-band-gap semiconductor that is widely employed as positive-electrode material in lithium-ion batteries.<sup>[2,6]</sup> The molecular redox shuttle (**S**) is dissolved in the electrolyte of the cathodic compartment of the cell. During charging **S** is oxidized at the current collector to **S**<sup>+</sup>, which delivers the charge to the LiFePO<sub>4</sub> particles by bulk diffusion. Because the standard redox potential of **S**<sup>+</sup> matches closely the Fermi level of LiFePO<sub>4</sub>, **S**<sup>+</sup> will be reduced back to **S** by hole injection in the LiFePO<sub>4</sub> particles, thus resulting in the oxidation of Fe<sup>II</sup> to Fe<sup>III</sup> and the release of lithium ions [Eq. (1)].



By contrast, during the discharging process, **S**<sup>+</sup> is reduced at the current collector to **S**, which in turn delivers electrons to FePO<sub>4</sub> [the reverse of Eq. (1)]. The advantage of using a freely diffusing redox shuttle over molecular wiring is that it allows charge transport to proceed at a much faster rate, thus enhancing greatly the power output of the battery.

In principle, any reversible redox couple whose standard Nernst potential closely matches the Fermi level of the battery material is suitable for the redox-targeting process. The present study employs osmium polypyridyl complexes as mediators. The Os<sup>II</sup>/Os<sup>III</sup> redox couple is stable and reversible, and electron exchange proceeds very rapidly (near the diffusion-limited rate) by an outer-sphere mechanism associated with a low reorganization energy. By changing the properties of the ligands, the redox potential can be readily tuned. Osmium complexes have been widely employed in electrochemical devices, such as sensors and bio-fuel cells,<sup>[7–9]</sup> as well as dye-sensitized solar cells and optoelectronic systems.<sup>[10–12]</sup>

The Os complexes [Os(mbpy)<sub>3</sub>]Cl<sub>2</sub> (**1**) and [Os(mobpy)<sub>3</sub>]Cl<sub>2</sub> (**2**) were used here for redox targeting of the



LiFePO<sub>4</sub> insertion material (mbpy = 4,4'-dimethyl-2,2'-bipyridine; mobpy = 4,4'-dimethoxy-2,2'-bipyridine). Figure 2 shows the cyclic voltammogram of a mixture of these two complexes measured with FTO (F-doped SnO<sub>2</sub>) coated conducting glass as the working electrode. Two reversible one-electron waves are observed; the formal potentials

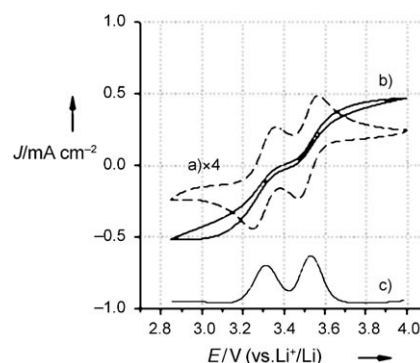


**Figure 2.** a,b) Cyclic voltammograms of a mixture of 4 mM [Os-(mbpy)<sub>3</sub>]<sup>2+</sup>/[Os(mobpy)<sub>3</sub>]<sup>2+</sup> in 1 M LiPF<sub>6</sub>/EC + EMC (1:1) electrolyte with FTO glass (a, dashed line) and carbon-free LiFePO<sub>4</sub> coated on FTO glass (b, solid line) electrodes. The current scale of (a) has been magnified by 4. The scan rate is 0.1 V s<sup>−1</sup>. c) Square-wave voltammogram obtained with the FTO electrode.

determined from square-wave voltammetry are 3.53 and 3.32 V (vs.  $\text{Li}^+/\text{Li}$ ) for **1** and **2**, respectively. The peak current is proportional to the square root of the scan rate (see the Supporting Information), which indicates the occurrence of a semi-infinite diffusion-controlled redox process.<sup>[13]</sup> The diffusion coefficients were calculated to be approximately  $1.5 \times 10^{-7} \text{ cm}^2 \text{ s}^{-1}$  for both complexes in the 1 M  $\text{LiPF}_6/\text{EC} + \text{EMC}$  (1:1, w/w) electrolyte (EC = ethylene carbonate; EMC = ethyl methyl carbonate). The redox potential for the two couples straddle the Fermi level of the  $\text{LiFePO}_4$  cathode material, which is about 3.45 V (vs.  $\text{Li}^+/\text{Li}$ ). Hence, on thermodynamic grounds,  $\text{LiFePO}_4$  can be oxidized to  $\text{FePO}_4$  by  $[\text{Os}(\text{mbpy})_3]^{3+}$  and the later reduced back by  $[\text{Os}(\text{mobpy})_3]^{2+}$ .

Unambiguous evidence for these redox processes is presented by the voltammogram in Figure 2b, for which the working electrode was a film of carbon-free  $\text{LiFePO}_4$  deposited on the FTO glass. In the absence of the redox relays, this electrode fails to exhibit any electrochemical response in the investigated potential range because of the insulating character of the  $\text{LiFePO}_4$  material. Strikingly, the addition of the two redox mediators produces two well-defined current plateaus for the oxidation and reduction processes. This result stands in marked contrast to the behavior with the bare FTO glass electrode, in which case the anodic and cathodic currents pass through peaks as a result of the growth of the diffusion layer. The appearance of the catalytic waves indicates that the two redox couples are recycled by charge injection in the battery material;  $[\text{Os}(\text{mbpy})_3]^{2+}$  is regenerated from  $[\text{Os}(\text{mbpy})_3]^{3+}$  by hole injection into the  $\text{LiFePO}_4$  layer and  $[\text{Os}(\text{mobpy})_3]^{3+}$  from  $[\text{Os}(\text{mobpy})_3]^{2+}$  by electron injection into the  $\text{FePO}_4$  layer during the charging and discharging, respectively. As a consequence, the current is not limited by the diffusion of the molecules and is around four times higher than that obtained with the FTO electrode alone. Furthermore, it was found that the plateau currents are almost independent of the scan rates (see the Supporting Information), which suggests finite-length diffusion behavior of the molecules confined in the pores of the electrode sheet.<sup>[14]</sup>

Following these encouraging results, a three-compartment electrochemical cell (shown in the Supporting Information) was used to charge and discharge the insulating  $\text{LiFePO}_4$  material. Each compartment of the cell was separated by a glass frit. A small quantity of the dark-brown electrolyte containing the two Os complexes was injected into the working-electrode compartment, and the other two compartments were filled with normal electrolyte. There was no appreciable leakage of the redox mediators across the frit during the experiments, which lasted for a few hours. Figure 3 depicts the voltage profiles of the electrodes during a galvanostatic charge and discharge cycle. Extended voltage plateaus were observed during the charge and discharge processes, which indicates that lithium extraction and insertion are sustained by the two redox relays. By contrast, no extended plateaus appear when bare FTO glass is used as a working electrode, because the  $[\text{Os}(\text{mbpy})_3]^{2+}$  and  $[\text{Os}(\text{mobpy})_3]^{3+}$  mediators are depleted by the oxidation and reduction processes, respectively. These results confirm that

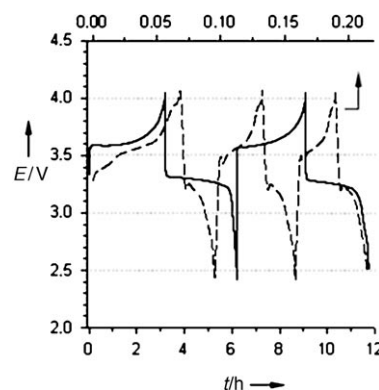


**Figure 3.** Voltage profiles of FTO (dashed line, top time axis) and carbon-free  $\text{LiFePO}_4/\text{FTO}$  (solid line, bottom time axis) electrodes obtained with a three-compartment electrochemical cell during galvanostatic charge/discharge processes. The electrolyte in the working-electrode compartment is 1 M  $\text{LiPF}_6/\text{EC} + \text{EMC}$  (1:1) containing 32 mM  $[\text{Os}(\text{mbpy})_3]^{2+}/[\text{Os}(\text{mobpy})_3]^{2+}$  with a volume of 30  $\mu\text{L}$ . The electrolytes in the other two compartments are 1 M  $\text{LiPF}_6/\text{EC} + \text{EMC}$  (1:1). The constant current is  $0.05 \text{ mA cm}^{-2}$ .

insulating  $\text{LiFePO}_4$  materials can be charged and discharged by using redox targeting by freely diffusing molecular relays even in the absence of conducting additives.

As well as by using two redox couples whose standard Nernst potentials straddle the Fermi level of the battery material, the redox targeting can also be effected by a single molecule. One example is 10-methylphenothiazine (MPTZ), whose standard potential is only slightly higher than that of  $\text{LiFePO}_4$ .<sup>[15]</sup> With an FTO electrode, the voltammogram (see the Supporting Information) shows the normal redox waves of MPTZ, the peak currents of which are limited by the semi-infinite diffusion MPTZ in electrolyte. By contrast, with the  $\text{LiFePO}_4$  electrode, the typical feature of a catalytic wave is again observed; the current plateaus show sustained oxidation and reduction processes resulting from molecular redox targeting. Thus, in the presence of MPTZ in the electrolyte, reversible lithium extraction/insertion involving the insulating  $\text{LiFePO}_4$  is possible.

It should be noted that in conventional batteries, the active electrode materials are in electronic contact with the current collector. The electrode materials are normally prepared with conducting additives to form an electrode sheet that is attached to a metal support. A novel configuration of a compact energy-storage system based on redox targeting may be conceived, as shown in Figure 4. The active electrode materials could be stored in separate tanks and electrochemically addressed by the redox relay surrounding them. These molecular redox shuttles establish the electronic communication between the local electrode material and the current collector. As no conducting additives are needed, the energy density is expected to be greatly improved. Moreover, with such configuration, the battery can be recharged by simply replacing the tanks with charged electrode materials, thus avoiding long charging times.

In summary, a novel concept to address battery materials electrochemically by using redox targeting has been introduced and demonstrated with  $\text{LiFePO}_4$  as an example. By

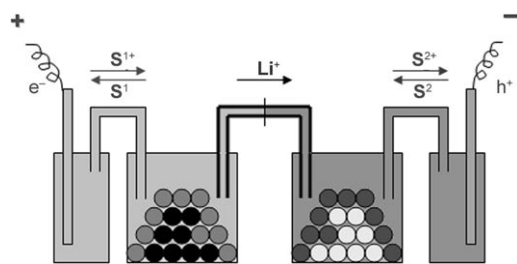


**Figure 4.** Configuration of a compact electric-energy-storage system. The active electrode materials are stored in tanks separated from the current collectors. The charges are transported between current collectors and active materials by the diffusion of molecular redox relays in the electrolyte.

using appropriate molecular shuttles, these concepts could be applied to other electrode materials, such as  $\text{LiCoO}_2$ ,  $\text{LiMnPO}_4$ ,  $\text{Li}_4\text{Ti}_5\text{O}_{12}$ , or even electrode materials for secondary batteries that do not employ lithium-insertion materials. In comparison with molecular wiring, larger power output can be expected for the targeting process. However, the challenge in this case is that a special separator has to be used to prevent the redox shuttle molecules from contacting the counter electrode, which leads to self-discharge. We propose that a solid  $\text{Li}^+$  conductor, such as lithium phosphorus oxynitride ( $\text{LiPON}$ ),<sup>[16]</sup>  $70\text{Li}_2\text{S} \cdot 30\text{P}_2\text{S}_5$ ,<sup>[17,18]</sup> and ceramic nanofiltration membranes<sup>[19]</sup> could be used for this purpose. Although such practical issues still need to be addressed, applications are feasible and offer opportunities for using insulating electrode materials in high-energy-storage systems.

## Experimental Section

The syntheses of  $[\text{Os}(\text{mbpy})_3]\text{Cl}_2$  and  $[\text{Os}(\text{mobpy})_3]\text{Cl}_2$  can be found in reference [8]. 10-Methylphenothiazine was purchased from Acros and used as received. These molecules were dissolved at different concentrations in an electrolyte of 1 M  $\text{LiPF}_6/\text{EC} + \text{EMC}$  mixture (1:1, w/w).

$\text{LiFePO}_4$  powder was synthesized by a solid-state reaction.<sup>[20]</sup> The electrode was prepared by mixing the  $\text{LiFePO}_4$  powder with 8 wt.% PVDF and stirring with *N*-methyl-2-pyrrolidone (NMP). The resulting homogeneous slurry was then doctor bladed onto FTO conducting glass. The films were dried in an oven at 100°C overnight, then cut into smaller pieces. The typical thickness of the film was 5–7  $\mu\text{m}$ .

Voltammetric and galvanostatic measurements employed a PC-controlled AutoLab PSTA30 electrochemical workstation (Eco Chimie) with counter and reference electrodes of lithium foil. The electrolyte was 1 M  $\text{LiPF}_6/\text{EC} + \text{EMC}$  (1:1, w/w).

Received: July 19, 2006

Published online: November 16, 2006

**Keywords:** electrochemistry · energy storage · lithium-ion batteries · redox chemistry

- [5] Q. Wang, N. Evans, S. M. Zakeeruddin, I. Exnar, M. Grätzel, *J. Am. Chem. Soc.* **2006**, submitted.
- [6] A. K. Padhi, K. S. Nanjundaswamy, J. B. Goodenough, *J. Electrochem. Soc.* **1997**, *144*, 1188–1194.
- [7] A. Heller, *J. Phys. Chem.* **1992**, *96*, 3579–3587.
- [8] S. M. Zakeeruddin, D. M. Fraser, M. K. Nazeeruddin, M. Grätzel, *J. Electroanal. Chem.* **1992**, *337*, 253–283.
- [9] F. Mao, N. Mano, A. Heller, *J. Am. Chem. Soc.* **2003**, *125*, 4951–4957.
- [10] R. Argazzi, G. Larramona, C. Contado, C. A. Bignozzi, *J. Photochem. Photobiol. A* **2004**, *164*, 15–21.
- [11] D. Kuciauskas, M. S. Freund, H. B. Gray, J. R. Winkler, N. S. Lewis, *J. Phys. Chem. B* **2001**, *105*, 392–403.
- [12] G. Sauve, M. E. Cass, S. J. Doig, I. Lauermaun, K. Pomykal, N. S. Lewis, *J. Phys. Chem. B* **2000**, *104*, 3488–3491.
- [13] A. J. Bard, L. R. Faulkner, *Electrochemical Methods: Fundamentals and Applications*, 2nd ed., Wiley, **2000**.
- [14] E. V. Milsom, H. R. Perrott, L. M. Peter, F. Marken, *Langmuir* **2005**, *21*, 9482–9487.
- [15] C. Buhrmester, L. Moshurchak, R. C. L. Wang, J. R. Dahn, *J. Electrochem. Soc.* **2006**, *153*, A288–A294.
- [16] S. D. Jones, J. R. Akridge, F. K. Shokoohi, *Solid State Ionics* **1994**, *69*, 357–368.
- [17] A. Hayashi, S. Hama, H. Morimoto, M. Tatsumisago, T. Minami, *J. Am. Ceram. Soc.* **2001**, *84*, 477–479.
- [18] R. Mercier, J. P. Malugani, B. Fahys, G. Robert, *Solid State Ionics* **1981**, *5*, 663–666.
- [19] S. Benfer, U. Popp, H. Richter, C. Siewert, G. Tomandl, *Sep. Purif. Technol.* **2001**, *22–3*, 231–237.
- [20] D. Y. Wang, L. Hong, Z. X. Wang, X. D. Wu, Y. C. Sun, X. J. Huang, L. Q. Chen, *J. Solid State Chem.* **2004**, *177*, 4582–4587.

[1] M. Winter, R. J. Brodd, *Chem. Rev.* **2004**, *104*, 4245–4269.

[2] J. M. Tarascon, M. Armand, *Nature* **2001**, *414*, 359–367.

[3] L. Aymard, C. Lenain, L. Courvoisier, F. Salver-Disma, J. M. Tarascon, *J. Electrochem. Soc.* **1999**, *146*, 2015–2023.

[4] J. K. Hong, J. H. Lee, S. M. Oh, *J. Power Sources* **2002**, *111*, 90–96.